Response Surface Methodology for the Optimization and Characterization of Oil Palm Mesocarp Fiber-graft-Poly(butyl acrylate)

Cher Chean Teh,[a] Nor Azowa Ibrahim,[a,]* and Wan Md Zin Wan Yunus [b]

Oil palm mesocarp fibers (OPMFs) are left as a waste material after oil extraction. A new application of OPMF is needed to economically utilize these fibers; thus OPMFs need to be modified to render them hydrophobic. Hydrogen peroxide was used to initiate the graft copolymerization of butyl acrylate onto OPMF in aqueous solution. The duration of reaction, temperature, and amounts of butyl acrylate and initiator were optimized using response surface methodology (RSM) coupled with a four-factor central composite design (CCD). The response variable was percentage grafting (%G). A quadratic model was obtained and developed to correlate the independent variables to %G. The optimum conditions predicted through RSM were 110 min duration of reaction, 50 °C temperature, 28 mmol of monomer, and 5.99 mmol of initiator, with a %G of 116.2%. Synthesized graft copolymers were characterized by Fourier-transform infrared spectroscopy (FTIR), scanning electron microscopy (SEM), and thermogravimetric analysis. The thermal stability of OPMF improved significantly after grafting. The FTIR and SEM results showed that graft copolymerization successfully occurred onto the OPMF backbone. The tensile test results support the utilization of grafted OPMF as a potential compatibilizer.

Keywords: Grafting; Response surface methodology; Copolymers; Fibers; Butyl acrylate

*Contact information: a: Department of Chemistry, Faculty of Science, Universiti Putra Malaysia, 43400 UPM Serdang, Selangor, Malaysia; b: Defence Science Department, Faculty of Defence Science and Technology, National Defence University of Malaysia, Sungai Besi Camp, 57000 Kuala Lumpur, Malaysia; *Corresponding author: norazowa@science.upm.edu.my*

INTRODUCTION

Remarkable development of oil palm industries has been observed in Malaysia. Currently, Malaysia is one of the biggest producers and exporters of palm oil and palm oil products. The oil palm industry creates an abundant amount of various oil palm fibers from fronds, trunks, mesocarp, empty fruit bunches, palm oil mill effluent, palm kernel cake, and palm press (Mohanty *et al*. 2005). Among the many types of oil palm biomass, OPMF have high potential as a reinforcing material in polymer composites. Usually, OPMF are mixed with other materials with high nitrogen contents to produce composted mass that can be used as organic fertilizer. In addition, the raw OPMF is used as boiler fuel to generate steam. However, it is expected that generation of OPMF will grow in the future, where the amount generated exceeds what can be burnt by the limited boiler capacity of the mills (Md Yunos *et al*. 2012). Therefore, it will be beneficial if these fibers can be fully utilized.

While going through the annals of literature, not much information is available on the application of OPMF as reinforcing material in the polymer composites. Keeping in

view the easy availability of this biomass, efforts have been made by our research group to discover new potential application of this fiber, particularly polymer composites reinforcement. OPMF consists of 60% cellulose and 11% lignin (Sreekala *et al*. 1997). Because of oily and dirty materials on the fiber surface, this fiber is still not exploited commercially for various end uses. Oil and dirt must be removed from the OPMF before it can be used. Like other natural fibers, OPMF suffers from a number of disadvantages, such as its hydrophilicity, susceptibility to biological attack, and low thermal stability (Hill 2006). Therefore, modification is needed to improve one or more of its disadvantages. Graft copolymerization is a well-established technique used for modifying or improving material properties for specific end uses (Kumar *et al*. 2007). There are many potential applications of graft copolymers, such as polymer composite reinforcement, support matrix in the removal of toxic metal ions, and green hydrogel supports by suitable functionalization as cation (Fe^{3+}) and anion (NO^{3-}) adsorbents (Thakur *et* al. 2011). Much research on graft copolymerization has been carried out on oil palm empty fruit bunch (OPEFB) fibers and other types of natural fibers as polymeric backbones (Raju *et al.* 2007; Thakur *et al.* 2012; Mahdavi *et al*. 2011). However, the utilization of OPMF in graft copolymer preparation has not yet been reported.

Natural fiber reinforced polymer composites produced from OPEFB fibers and new cellulosic materials have offered some specific properties that can be comparable to conventional synthetic fiber composite materials (Singha and Thakur 2008; Hassan *et al*. 2010; Abu Bakar and Baharulrazi 2008; Singha and Thakur 2009; Singha and Thakur 2010). Therefore, it appears that OPMF as a reinforcing material for polymers is a potential application. In fact, grafted fiber can be used as a reinforcing agent in a poly(lactic acid) (PLA) matrix to enhance the mechanical properties and thermal stability and to reduce costs (Madhavan *et al*. 2010). Poly(butyl acrylate) (PBA) was chosen here to modify OPMF because PBA is more compatible than OPMF with PLA due to the interactions of both materials' ester groups (Qin *et al*. 2011).

Optimization through RSM has been widely applied in many experimental situations: using a mathematical relationship to describe the response of interest in terms of the independent variables being studied, an approximating model can be obtained and the optimum conditions can be determined (Jyothi *et al*. 2010).

In the conventional 'one-variable-at-a-time' approach, the factors are optimized by changing one factor at a time and keeping other variables constant. However, this method is time-consuming and does not take into account the interactive effects among the factors studied. RSM is capable of simultaneously determining the individual and interactive effects of many factors of interest and reduces the total required experimental runs (Razali *et al*. 2012). Therefore, optimization of the reaction parameters was carried out using RSM.

The aim of the present study was to optimize the reaction parameters to maximize the %G of OPMF-graft-poly(butyl acrylate) using H_2O_2/Fe^{2+} as a redox initiator in an aqueous medium. Subsequently, the synthesized graft copolymers were used for the preparation of biocomposites.

Central composite design (CCD) is a response surface method that can fit a quadratic surface, which works well for process optimization. In this study, a CCD was proposed because this design can fit the true response surface that would be required for determination of the optimal conditions.

EXPERIMENTAL

Materials

Oil palm mesocarp fiber (OPMF) was received from Felda Palm Industries Sdn Bhd palm oil mills in Negeri Sembilan state. The fibers were ground and sieved to a size less than 150 µm. The OPMF powder was soaked for 6 h and washed first with hot water, then with acetone, and then dried in oven at 60 °C to constant weight. Butyl acrylate (BA) was obtained from Sigma Aldrich (USA) and purified by passing it through a column packed with activated alumina to remove its inhibitors. Hydrogen peroxide solution (2 M) was prepared from analytical-grade hydrogen peroxide, purchased from Merck (Germany). Analytical-grade ammonium iron(II) sulfate hexahydrate was obtained from Merck (Germany) and used as received. PLA (4042D commercial grade) in pellet form was supplied by NatureWorks® (LCC, Minnesota, USA). Solvents and other chemicals of analytical grade were used as received from manufacturers.

Synthesis of OPMF-g-copolymer

A four-factor five-level response surface CCD, which requires 30 runs, including six replicates of the central run, eight axial runs, and 16 factorial runs, was used for the synthesis and optimization of graft copolymers of OPMF with BA using H_2O_2/Fe^{2+} as a redox initiator in an aqueous medium. Table 1 shows the range of the independent variables and experiment design levels used in this work. The four factors and their ranges were chosen based on preliminary studies. The responses were fitted to the quadratic regression models, as shown below, in terms of the variables selected,

$$Y = \beta_0 + \sum_{i=1}^{k} \beta_i x_i + \sum_{i=1}^{k} \beta_{ii} x_i^2 + \sum_{i<j}^{k} \beta_{ij} x_i x_j + \varepsilon \quad (1)$$

where Y represents the responses (dependent variables), β_0 is the constant coefficient, and β_i, β_{ii}, and β_{ij} are coefficients for the linear, quadratic, and interaction effects, respectively. x_i and x_j are factors (independent variables), and ε is the experimental error. The factors were coded in levels (-2, -1, 0, +1, +2) before fitting the model.

Table 1. Experimental Range and Levels of the Respective Independent Variables

			Coded Level				
Variable	Notation	Unit	-2	-1	0	1	2
Time	(A)	min	100	110	120	130	140
Temperature	(B)	°C	30	40	50	60	70
Monomer	(C)	mmol	7	14	21	28	35
Initiator	(D)	mmol	2	4	6	8	10

The synthesis was based on the procedure of Ibrahim *et al*. (2003a). One gram of dried OPMF (< 150 µm) was added to 100 mL of distilled water in a 250-mL three-necked flask. The flask was kept in a water bath at the chosen temperature. Nitrogen gas was bubbled through the slurry. After 30 min, the required volume of 2.0 M H_2O_2 and the required amount of ammonium iron(II) sulfate were added. The solution was kept for about 5 min to facilitate free radical formation. Then, the required amounts of BA were

added, and the reaction mixture was stirred for the required time. At the end of the period, the flask was cooled under running tap water and the product was filtered. The crude product was washed thoroughly with distilled water and oven dried at 60 °C to constant weight.

Removal of Homopolymer and Determination of Graft Level

The crude product was purified with tetrahydrofuran using a Soxhlet extractor for 24 h to remove the homopolymer and remaining monomer. The pure grafted copolymers were then dried at 60 °C to constant weight. The percentage grafting was calculated as follows,

$$\text{Percentage grafting (\%G)} = \left[\frac{(W_1 - W_0)}{W_0}\right] \times 100 \quad (2)$$

where W_0 and W_1 denote the weights (in grams) of the original OPMF and grafted OPMF after extraction, respectively.

Preparation of Composites

The synthesized graft copolymers with %G = 116.2% were used to prepare PLA biocomposites. The ratio of PLA/OPMF was fixed at 60:40 and five different loadings (0, 1, 2, 3, 4, or 5%) of OPMF-*graft*-PBA were used. The PLA, OPMF, and OPMF-*graft*-PBA were weighted at the desired addition level and premixed in a glass beaker. The mixture was then melt-compounded in a Thermo Haake Polydrive internal mixer at 170 °C for 10 min at a mixing speed of 50 rpm. These compounded materials were then compressed into 1 mm thick film by hydraulic hot-press at 160 °C under pressure of 110 kg/cm^2 for 5 min, followed by cooling to room temperature. Composites thus prepared were subjected to tensile testing. The tensile test was carried out by a Universal Testing Machine, Instron 4302, according to ASTM D638-5. A load of 1.0 kN was applied at constant crosshead speed of 10 mm/min at room temperature. Five specimens were used for tensile testing.

FTIR Analysis

Infrared spectra of the OPMF and grafted OPMF were recorded on a Perkin Elmer Spectrum 1000 Series spectrophotometer equipped with attenuated total reflectance (ATR). The infrared spectra were recorded in the range of frequency of 4000 to 400 cm^{-1}.

Thermogravimetric Analysis (TGA)

Thermogravimetry experiments were carried out using a Metler Toledo Thermal Analyzer from 35 °C to 600 °C at a heating rate of 10 °C/min with a nitrogen flow rate of 50 mL/min.

Scanning Electron Microscopy (SEM) Examination

The scanning electron micrographs of OPMF, OPMF-*graft*-PBA, and tensile fracture surface of biocomposites samples were recorded by a JEOL (Model JSM-6400) scanning electron microscope operating at 15 kV. The samples were coated with gold to enhance conductivity.

Statistical Analysis

The data were analyzed using Design-Expert software (version 8.0.6). Analysis of variance (ANOVA) was employed to determine the interaction effects between the factors, and a quadratic surface plot was generated. The adequacy of the model was tested using ANOVA, a normal probability plot, and a residual plot (Chieng *et al.* 2012). An F-test was used to determine the statistical significance of the model and the significance of the regression coefficients.

RESULTS AND DISCUSSION

Statistical Analysis of Results and Model Fitting

The samples were synthesized under different reaction variable conditions, and the experimental data are presented in Table 2. The %G of the grafted OPMF ranged from 1.0 to 185.3%. The highest %G of 185.3% was synthesized under the following conditions: time = 120 min, temperature = 50 °C, amount of monomer = 35 mmol, and amount of initiator = 6 mmol.

Table 2. Experimental Design and Actual Response of Percentage Grafting

Run no.	Variables in decoded levels				Actual response
	Time (min) (A)	Temperature (°C) (B)	Monomer (mmol) (C)	Initiator (mmol) (D)	Percentage grafting (%)
1	130	60	14	4	12.19
2	130	40	28	4	80.09
3	120	50	21	6	74.13
4	100	50	21	6	59.34
5	120	50	35	6	185.3
6	120	50	21	2	13.76
7	120	50	21	6	74.52
8	110	40	28	4	69.24
9	110	40	28	8	102.73
10	110	60	14	8	21.61
11	120	50	21	6	75.15
12	130	40	28	8	114.91
13	120	70	21	6	68.79
14	120	30	21	6	32.54
15	140	50	21	6	72.87
16	130	60	28	8	153.14
17	110	40	14	4	11.09
18	120	50	21	6	76.22
19	120	50	7	6	1.04
20	110	40	14	8	16.98
21	120	50	21	6	73.98
22	130	60	28	4	106.29
23	130	40	14	8	16.14
24	120	50	21	10	63.09
25	110	60	28	8	136.04
26	120	50	21	6	76.14
27	110	60	28	4	93.38
28	130	40	14	4	12.19
29	110	60	14	4	11.31
30	130	60	14	8	22.74

A quadratic model was found to fit adequately to the experimental data ($p < 0.05$). The experimental response can be modeled as a polynomial equation that shows the effect of reaction variables on the %G through the estimation of regression coefficients. The quadratic function in terms of coded factors is given as follows (Soo *et al*. 2012):

$$\% \text{ Grafting} = +75.02 + 3.43A + 8.58B + 45.84C + 11.97D + 0.55AB + 3.17AC + 0.24AD + 6.90BC + 2.01BD + 7.95CD - 2.37A^2 - 6.23B^2 + 4.40C^2 - 9.29D^2 \quad (3)$$

The ANOVA for the quadratic model is presented in Table 3. The linear and quadratic terms of all four variables have significant effects on percentage grafting ($p \leq 0.05$). The interaction terms AB and AD are not statistically significant, as indicated by p values greater than 0.10. The lack of fit test is a test indicating the significance of the replicate error in comparison to the model dependent error. The lack of fit test in this study is not significant relative to pure error, as the F-ratio for lack of fit is not significant (Ghafari *et al*. 2009).

Table 3. ANOVA of the Response Surface Quadratic Model for Percentage Grafting

Source	Sum of Squares	Df	Mean Square	F Value	p-value Prob > F	
Quadratic	62131.70	14	4437.98	2488.81	< 0.0001	Significant
A-Time	282.70	1	282.70	158.54	< 0.0001	
B-Temperature	1765.25	1	1765.25	989.95	< 0.0001	
C-Monomer	50424.92	1	50424.92	28278.20	< 0.0001	
D-Initiator	3436.11	1	3436.11	1926.96	< 0.0001	
AB	4.76	1	4.76	2.67	0.1230	
AC	161.10	1	161.10	90.34	< 0.0001	
AD	0.92	1	0.92	0.51	0.4844	
BC	762.17	1	762.17	427.43	< 0.0001	
BD	64.84	1	64.84	36.36	< 0.0001	
CD	1010.13	1	1010.13	566.48	< 0.0001	
A^2	153.94	1	153.94	86.33	< 0.0001	
B^2	1064.26	1	1064.26	596.84	< 0.0001	
C^2	530.34	1	530.34	297.41	< 0.0001	
D^2	2366.72	1	2366.72	1327.25	< 0.0001	
Residual	26.75	15	1.78			
Lack of Fit	21.91	10	2.19	2.27	0.1897	Not significant
Pure Error	4.83	5	0.97			
Cor Total	62158.45	29				
Std. Dev.	1.34		R-Squared		0.9996	
Mean	64.23		Adj R-Squared		0.9992	
C.V. %	2.08		Pred R-Squared		0.9979	
PRESS	133.18		Adeq. Precision		194.176	

The coefficient of multiple determination (R^2) value was 0.9996. That is, the quadratic model explains about 99.96% of the variability observed in the %G. When R^2 and adjusted R^2 (R^2_{adj}) differ dramatically, there is a good chance that non-significant terms have been included in the model. The adjusted R^2 of 0.9992 reveals no apparent problem. In addition, the standard deviation and prediction error sum of squares (PRESS) were 1.34 and 133.18, respectively. A low standard deviation and low PRESS indicate that the quadratic model can be fit adequately to the experimental data. The difference between adjusted R^2 and predicted R^2 is < 0.2, and the model adequate precision is 194.18, which also indicates that the model is adequate (Chieng *et al*. 2012).

In addition, the adequacy of the model was also investigated by residual analysis. A check of the normality assumption may be made by examining a normal probability plot of the residuals, as in Fig. 1. If the residuals plot approximately along a straight line, then the normality assumption is satisfied (Myers *et al*. 2009). The residuals plot reveals no apparent problem with normality. Figure 2 shows a plot of residuals versus the predicted response for %G. Residuals are randomly scattered around the mean of the response variable. This implies that the quadratic model proposed was adequate.

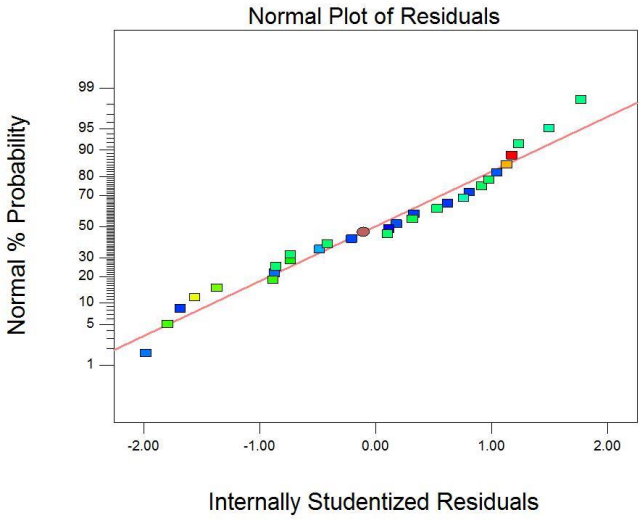

Fig. 1. Normal probability plot of residuals

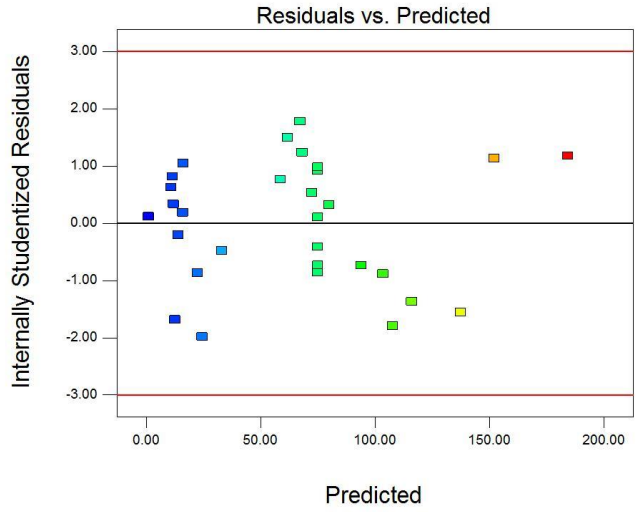

Fig. 2. Plot of residuals versus predicted response

Effect of Reaction Variables on Grafting

The results showed that higher levels of all the factors favored the grafting reaction. The coefficients for the main effects were significant and positive (Eq. 3), which indicates an increase in %G for unit change in the corresponding reaction variables. However, the negative sign for the coefficients of the quadratic effects of time, temperature, and initiator indicate that there is a decrease in %G after reaching an optimum (Jyothi *et al*. 2010). These trends can be visualized in the three dimensional surface plots for the %G shown in Fig. 3.

The %G increased with the increased amounts of monomer from 14 to 28 mmol, as shown in Fig. 3(b), (d), and (f). This is because more monomers are available and can react with the grafting sites in the OPMF (Thakur *et al*. 2013). The effects of the reaction duration on %G are shown in Fig. 3(a), (b), and (c). The percentage grafting increased with an increase in reaction time during the earlier reaction period and leveled off after 2 h. In contrast, Abu-Ilaiwi *et al*. (2003) reported that the %G decreases significantly after the optimum reaction time, which was 60 min. The result of the %G after 2 h was expected because there were no more active sites for monomers to react, thus resulting in diffusion retardation.

The effects of squared temperature and the amount of initiator on %G are depicted in Fig. 3(e). The results are in agreement with the earlier report of Thakur *et al*. (2011), who observed that %G increased with the initial increase in temperature, up to 45 °C, and then decreased with a further rise in temperature. As the kinetic energy of the molecules increases due to an increase in temperature, more radicals drifted at a faster rate onto the backbone, resulting in the increase of %G. However, a further increase in temperature lead to too many free radicals, thus the radicals initiate homopolymerization, which results in the decrease in %G.

The quadratic effect of initiators can also be explained, as follows: the initial rise in %G may be due to the increase in the number of free radical sites on the OPMF backbone, and the decrease in %G may be due to the enhanced rate of termination and the initiation of homopolymerization.

The perturbation plot, Fig. 4, shows the effect of each factor as it moves from the reference point, with all other factors held constant at the reference value. The reference value was: time = 120 min, temperature = 50 °C, amount of monomer = 21 mmol, and amount of initiator = 6 mmol. When the factor curvature is sharper, the factor effect is more important to the response (Konwarh *et al*. 2013). The %G was most sensitive to the amount of monomer followed by amount of initiator, temperature, and finally by the reaction time.

The effects of squared reaction time, temperature, and initiator amount were demonstrated in Fig. 4(a), (b), and (d), where the %G decreased or leveled off after reaching an optimum. From Fig. 4(a), the optimum time of grafting was found to be 120 min. The %G leveled off with a further increase in time.

From Fig. 4(b), the %G increased with an increase in the temperature, and reached a maximum value of about 78% at 56 °C. A further increase in temperature was accompanied by a slow decrease in the %G. In addition, the %G increased with an increase in the initiator amount and reached a maximum value of about 80%, at 7.3 mmol of initiator. A further increase in initiator amount was accompanied by a slow decrease in the %G.

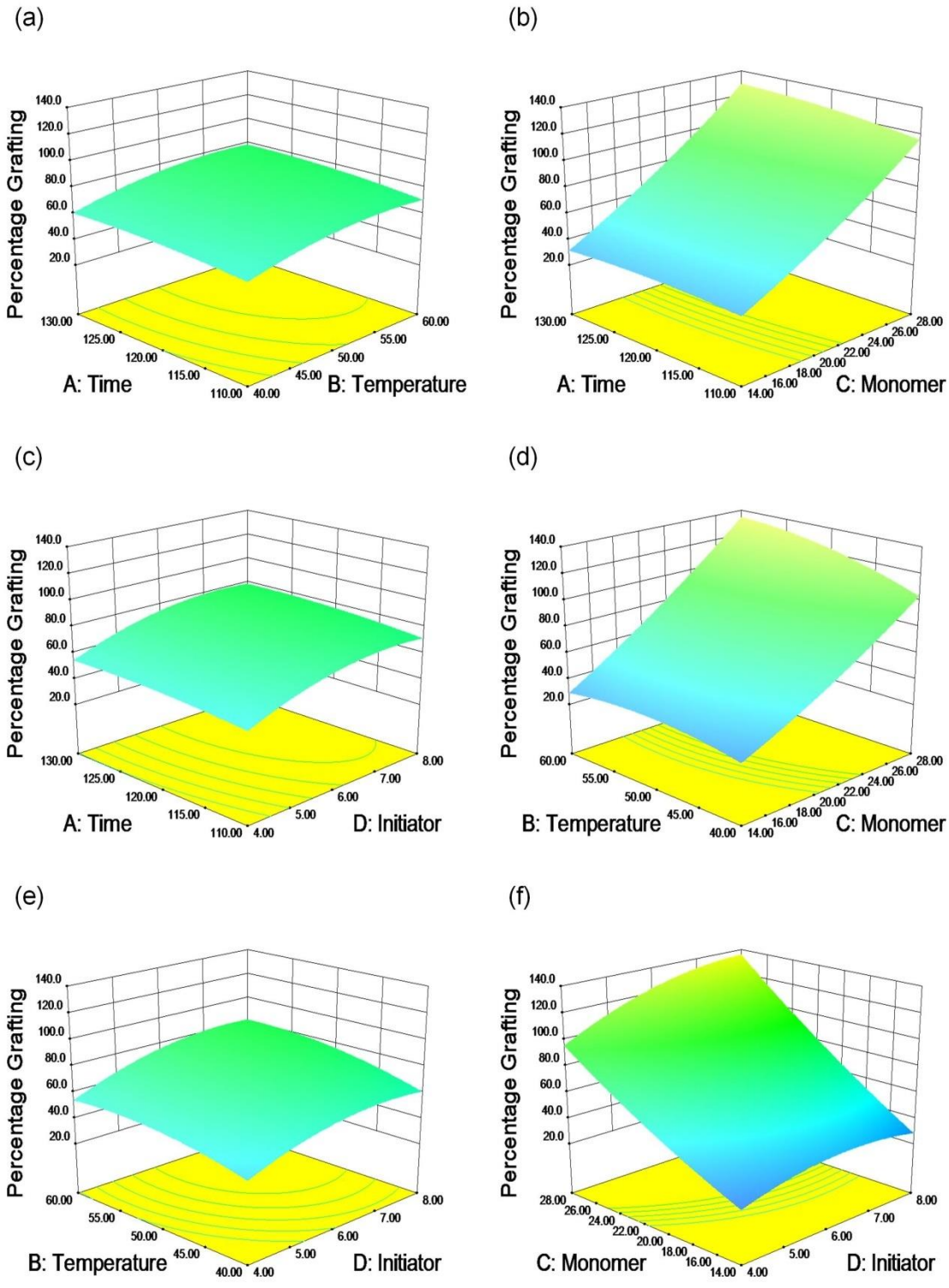

Fig. 3. Three-dimensional response surface plot of percentage grafting as a function of (a) time and temperature, (b) time and monomer, (c) time and initiator, (d) temperature and monomer, (e) temperature and initiator, and (f) monomer and initiator

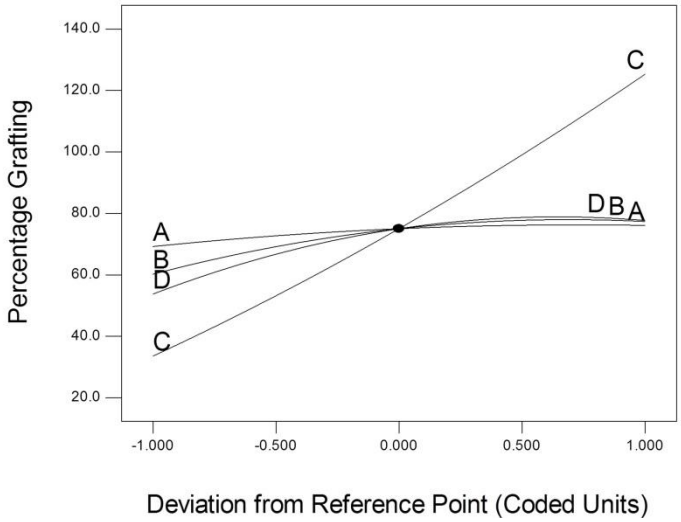

Fig. 4. Perturbation plot for percentage grafting: (a) reaction time, (b) temperature, (c) monomer amount, and (d) initiator amount

Optimization of Percentage Grafting

The optimum conditions for obtaining the maximum %G were predicted using the quadratic model. The goals were set as shown in Table 4. The first 10 predicted combinations are shown in Table 5. The number 1 combination was chosen because it achieved the highest desirability (0.699). In addition, the optimum time to get maximum grafting was 10 min shorter as compared to the previous study conducted by Ibrahim *et al.* (2003b).

Table 4. Constraints Applied for Optimization

Name	Goal	Lower limit	Upper limit
Time, min	Minimize	110	130
Temperature, °C	Is in range	40	50
Monomer, mmol	Is in range	14	28
Initiator, mmol	Is in range	4	6
Percentage grafting, %	Maximize	50	185.3

Table 5. Optimum Combinations for Optimization of Percentage Grafting

No.	Time (min)	Temperature (°C)	Monomer (mmol)	Initiator (mmol)	Percentage grafting (%)	Desirability	
1	110.00	50.00	28.00	5.99	116.2	0.699	Selected
2	110.00	49.78	28.00	6.00	115.9	0.698	
3	110.00	50.00	27.92	6.00	115.7	0.697	
4	110.00	49.42	28.00	6.00	115.4	0.695	
5	110.00	49.07	28.00	6.00	114.8	0.692	
6	110.72	50.00	27.99	6.00	117.0	0.691	
7	110.00	50.00	28.00	5.83	114,6	0.691	
8	110.00	48.72	27.99	6.00	114.2	0.689	
9	110.00	48.57	28.00	6.00	114.0	0.688	
10	110.00	50.00	27.68	6.00	113.9	0.687	

To confirm the model, three additional experiments were performed under the chosen condition. Table 6 shows the reported runs using the number 1 combination. The percentage of error between the predicted value and experimental data was less than 2%. This also suggests the validity of the response model.

Table 6. Results of Validated Experiment Conducted at Optimum Condition

No.	Time (min)	Temperature (°C)	Monomer (mmol)	Initiator (mmol)	Percentage grafting (%)		Error (%)
					Predicted	Experimental	
1	110	50	28	5.99	116.2	116.8	0.52
2	110	50	28	5.99	116.2	118.1	1.64
3	110	50	28	5.99	116.2	117.4	1.03

FTIR Analysis

Grafting onto OPMF was confirmed by comparing the FTIR spectra of the OPMF with those of the grafted OPMF, as shown in Fig. 5.The FTIR spectrum of the raw OPMF shows O-H stretching vibration at 3342 cm^{-1}, C-H stretching at 2918 cm^{-1}, C=O stretching vibration at 1725 cm^{-1}, a bending mode of the adsorbed water at 1608 cm^{-1}, and C-O-C stretching vibrations at 1243 and 1030 cm^{-1} (Sayyah *et al*. 2013). The absorptions around 1369 and 1445 cm^{-1} appeared due to C-C bending vibrations. The spectrum of the grafted OPMF also showed all the peaks characteristic of the OPMF backbone. The reduction of the O-H broad peak shows that grafting successfully took place (Bakar *et al*. 2008). The presence of two new peaks at 2956 and 2875 cm^{-1} indicates the presence of the aliphatic chain from poly(butyl acrylate) (Ibrahim *et al*. 2003b). The increase in intensity of the C=O peak at 1729 cm^{-1} in the spectrum of grafted OPMF indicates the presence of the ester carbonyl group from BA and provides strong evidence of grafting (Kaith *et al*. 2009). In addition, the new peaks that appeared at 841 and 740 cm^{-1} were due to stretching of the CH_2CH_2 group and also provide evidence of grafting.

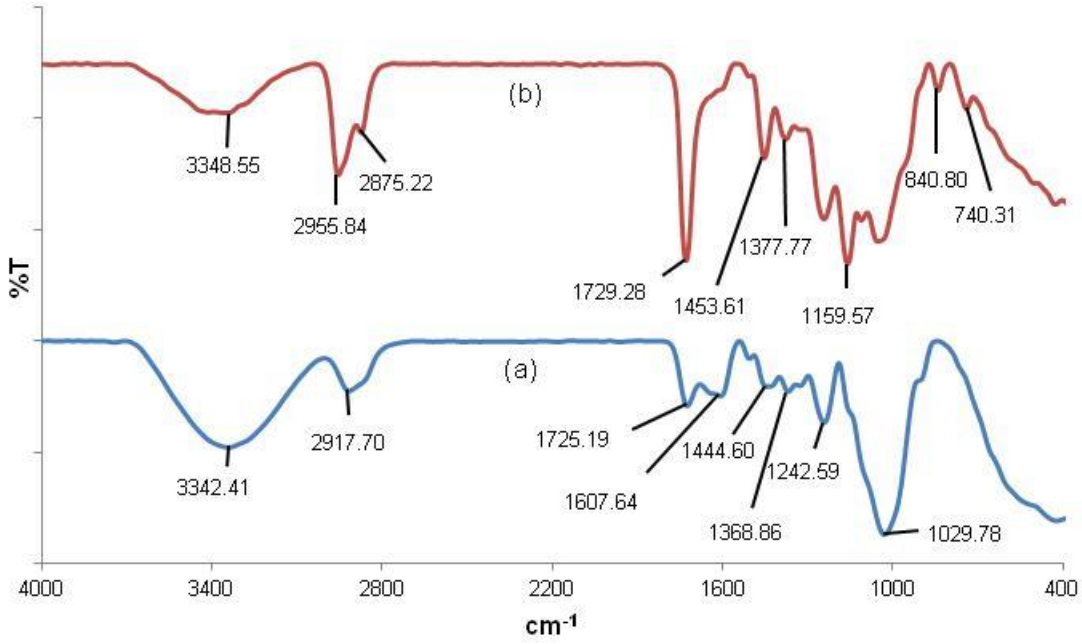

Fig. 5. Infrared spectra of (a) OPMF and (b) OPMF-*graft*-poly(butyl acrylate) with %G = 116.2%

Scanning Electron Microscopy

SEM micrographs of ungrafted and grafted OPMF are shown in Fig. 6. These micrographs clearly show the difference in their surface morphology. The ungrafted OPMF surface was rough, with protruding portions and groove-like structures, which may be due to the removal of fiber waxes and fats. The grafted fiber was homogeneously covered by poly(butyl acrylate) (Thakur *et al*. 2012). SEM micrographs provided morphological evidence for the grafting of BA onto OPMF. The adsorption and coating of PBA on OPMF was a good indication for biocomposite preparation (Qin *et al*. 2011). PBA, which was hydrophobic, was expected to improve the compatibility of the hydrophilic OPMF with the hydrophobic polymer.

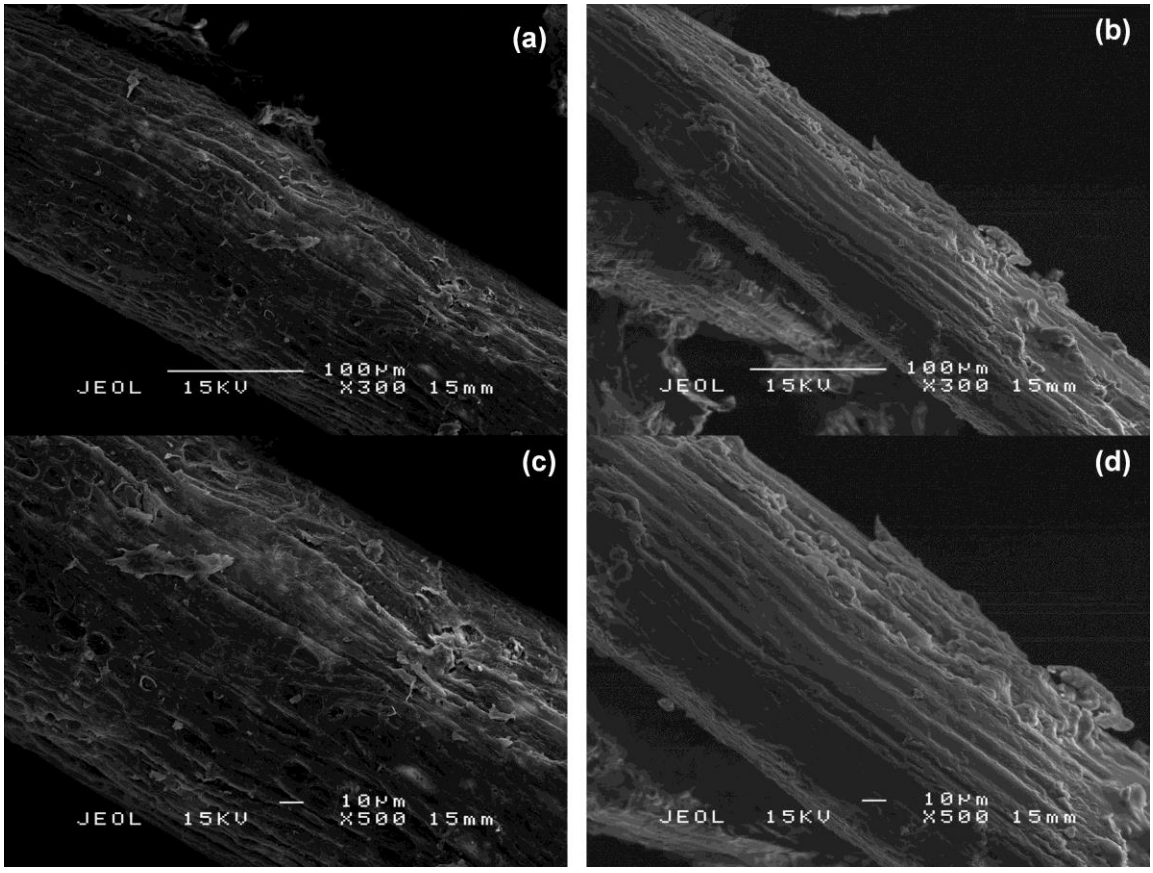

Fig. 6. Scanning electron micrographs of the ungrafted and grafted OPMF: (a) ungrafted OPMF(x 300), (b) OPMF-*graft*-poly(butyl acrylate) with %G = 116.2% (x 300), (c) ungrafted OPMF (x 500), (d) OPMF-*graft*-poly(butyl acrylate) with %G = 116.2% (x 500)

Thermogravimetric Analysis

The TGA thermograms of OPMF and OPMF-*graft*-PBA are shown in Fig. 7. In the case of ungrafted OPMF, a mass loss of 8.88% below 100 °C indicates the loss of moisture from the fibers. It can be observed that 58.37% of the weight loss from 200 to 380 °C was due to the decomposition of hemicelluloses, cellulose, and lignin (Yang *et al*. 2007). The weight loss after 380 °C may be due to the decomposition of lignin. The significant reduction of moisture content weight loss below 100 °C indicates that the grafted fibers become hydrophobic in nature as a result of grafting. The decomposition of

OPMF-graft-PBA occurred at 226 to 482 °C, with a weight loss of 83.10%. This clearly shows that thermal stability was increased with the grafting process (Thakur *et al.* 2012).

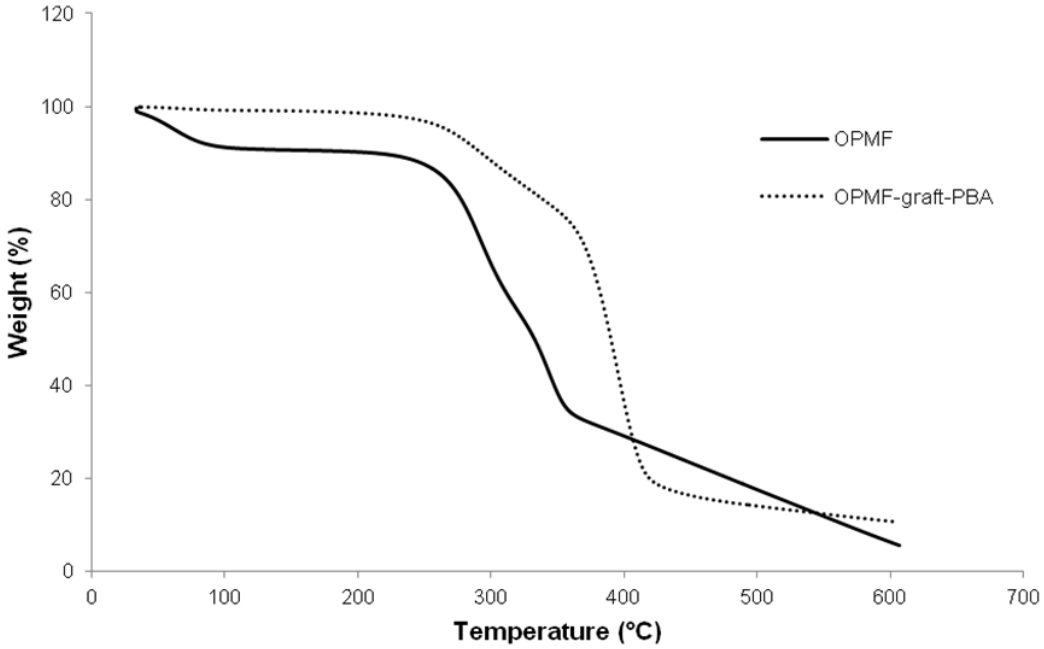

Fig. 7. TGA thermograms of OPMF and OPMF-*graft*-poly(butyl acrylate) with %G = 116.2%

Tensile Properties

The tensile strength and elongation at break of the composites was examined, as shown in Fig. 8.

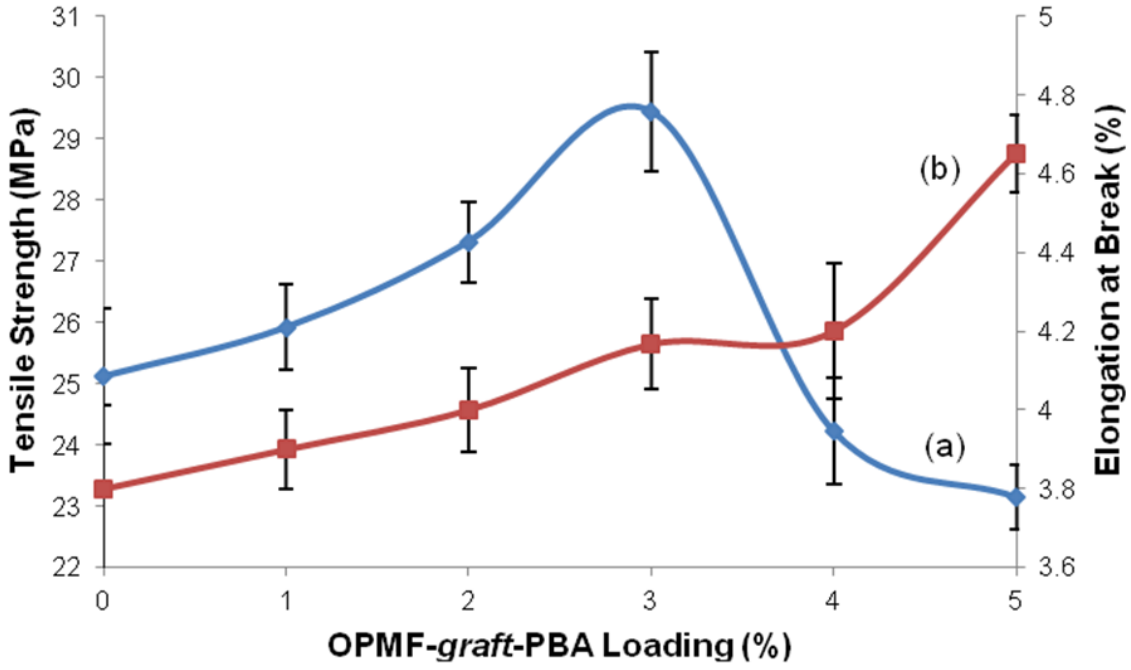

Fig. 8. Relationship between tensile property and loading of OPMF-*graft*-PBA: (a) tensile strength (MPa) and (b) elongation at break (%)

The tensile strength increased with the increase of the OPMF-*graft*-PBA loading from 0 to 3%. The tensile strength of PLA/OPMF/3% OPMF-*graft*-PBA composite increased by about 5 MPa compared to the composite with 0% OPMF-*graft*-PBA. In addition, the elongation at break increased slowly from 0 to 5%. These were attributed to the PBA adsorbed on the fiber surface and good interfacial adhesion between OPMF-*graft*-PBA and PLA matrix (Qin *et al.* 2011). However, beyond 3%, the tensile strength decreased. This might be due to the poor dispersion of excess PBA and causes stress defects which reduced the strength. Therefore, this implies that the OPMF-*graft*-PBA may function as a compatibilizer.

Morphology of Composites

The fracture surface morphology of PLA/OPMF/OPMF-*graft*-PBA composites was analyzed by SEM, as shown in Fig. 9. It can be seen in Fig. 9(a) that for PLA/OPMF/0% OPMF-*graft*-PBA, some cavities were left by the pulled out fibers. Moreover, the fiber was loosely embedded and detached in the matrix. This indicates poor adhesion between PLA and OPMF. Figure 9(b) clearly shows that the compatibilizing effect of OPMF-*graft*-PBA gave rise to the fiber breakage at the fracture surface. This indicates good interfacial adhesion between the fiber and PLA matrix. This might be attributed to the chemical structure and degree of functional groups of grafted fiber improves the interaction between the phases of the composites (Qin *et al.* 2011). From Fig. 9(c), lumps of PBA can be observed which was due to the poor compatibility between PLA and PBA when OPMF-*graft*-PBA loading was more than 3%. Excessive PBA were agglomerated in the matrix and induced the poor interfacial adhesion.

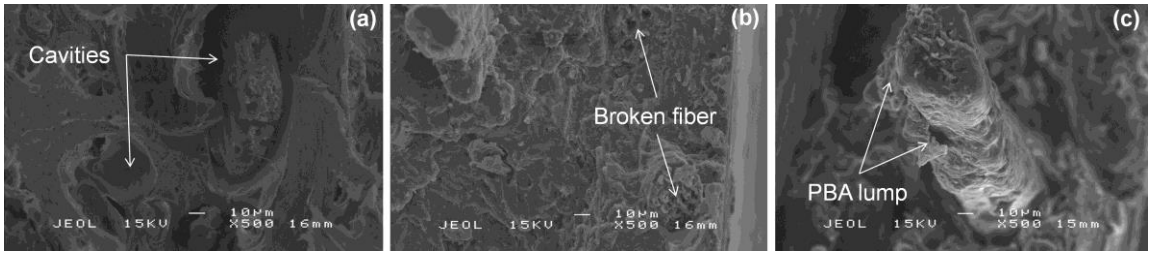

Fig. 9. SEM images of (a) PLA/OPMF/0% OPMF-*graft*-PBA, (b) PLA/OPMF/3% OPMF-*graft*-PBA, and (c) PLA/OPMF/5% OPMF-*graft*-PBA biocomposites

CONCLUSIONS

1. The OPMF-graft-poly(butyl acrylate) was successfully synthesized by H_2O_2/Fe^{2+}-initiated polymerization of OPMF with BA. The predicted optimum conditions were 110 min reaction duration, 50 °C temperature, 28 mmol of monomer, and 5.99 mmol of initiator, with a %G of 116.2%.
2. FTIR and SEM indicated that PBA was adsorbed and coated on OPMF. The thermal stability of OPMF improved significantly after grafting. These suggested that graft copolymerization is a good method for the surface modification of OPMFs.
3. The tensile test results suggest that OPMF-graft-PBA can act as a compatibilizer for PLA/OPMF composites.

REFERENCES CITED

Abu Bakar, A., and Baharulrazi, N. (2008). "Mechanical properties of benzoylated oil palm empty fruit bunch fiber reinforced poly(vinyl chloride) composites," *Polym-Plast. Technol.* 47(10), 1072-1079.

Abu-Ilaiwi, F. A., Ahmad, M. B., Ibrahim, N. A., Ab. Rahman, M. Z., Md. Dahlan, K. Z., and Yunus, W. Md. Z. W. (2003). "Graft copolymerization of methyl methacrylate onto rubber-wood fiber using H_2O_2 and Fe^{2+} as an initiator system," *J. Appl. Polym. Sci.* 88(10), 2499-2503.

Bakar, A. A., Mat, N. S. N., and Isnin, M. K. (2008). "Optimized conditions for the grafting reaction of poly(methyl methacrylate) onto oil-palm empty fruit bunch fibers," *J. Appl. Polym. Sci.* 110(2), 847-855.

Chieng, B. W., Ibrahim, N. A., and Wan Yunus, W. M. Z. (2012). "Optimization of tensile strength of poly(lactic acid)/graphene nanocomposites using response surface methodology," *Polym-Plast. Technol.* 51(8), 791-799.

Ghafari, S., Aziz, H. A., Isa, M. H., and Zinatizadeh, A. A. (2009). "Application of response surface methodology (RSM) to optimize coagulation–flocculation treatment of leachate using poly-aluminum chloride (PAC) and alum," *J. Hazard. Mater.* 163(2-3), 650-656.

Hassan, A., Salema, A. A., Ani, F. N., and Abu Bakar, A. (2010). "A review on oil palm empty fruit bunch fiber-reinforced polymer composite materials," *Polym. Composite* 31(12), 2079-2101.

Hill, C. A. S. (2006). *Wood Modification: Chemical, Thermal and Other Processes*, C. V. Stevens (ed.), John Wiley & Sons, New York.

Ibrahim, N. A., Wan Yunus, W. M. Z., Abu-Ilaiwi, F. A., Rahman, M. Z. A., Ahmad, M. B., and Dahlan, K. Z. M. (2003a). "Graft copolymerization of methyl methacrylate onto oil palm empty fruit bunch fiber using H_2O_2/Fe^{2+} as an initiator," *J. Appl. Polym. Sci.* 89(8), 2233-2238.

Ibrahim, N. A., Wan Yunus, W. M. Z., Abu-Ilaiwi, F. A. F., Rahman, M. Z. A., Ahmad, M. B., and Dahlan, K. Z. M. (2003b). "Optimized condition for grafting reaction of poly(butyl acrylate) onto oil palm empty fruit bunch fibre," *Polym. Int.* 52(7), 1119-1124.

Jyothi, A. N., Sreekumar, J., Moorthy, S. N., and Sajeev, M. S. (2010). "Response surface methodology for the optimization and characterization of cassava starch-graft-poly(acrylamide)," *Starch – Starke* 62(1), 18-27.

Kaith, B. S., Jindal, R., and Maiti, M. (2009). "Induction of chemical and moisture resistance in *Saccharum spontaneum* L. fiber through graft copolymerization with methyl methacrylate and study of morphological changes," *J. Appl. Polym. Sci.* 113(3), 1781-1791.

Konwarh, R., Misra, M., Mohanty, A. K., and Karak, N. (2013). "Diameter-tuning of electrospun cellulose acetate fiber: A Box-Behnken design (BBD) study," *Carbohyd. Polym.* 92(2), 1100-1106.

Kumar, R., Srivastava, A., and Behari, K. (2007). "Graft copolymerization of methacrylic acid onto xanthan gum by Fe^{2+}/H_2O_2 redox initiator," *J. Appl. Polym. Sci.* 105(4), 1922-1929.

Madhavan Nampoothiri, K., Nair, N. R., and John, R. P. (2010). "An overview of the recent developments in polylactide (PLA) research," *Bioresour. Technol.* 101(22), 8493-8501.

Mahdavi, M., Ahmad, M. B., Haron, M. J., Ab. Rahman, M. Z., and Fatehi, A. (2011). "Optimized conditions for graft copolymerization of poly(acrylamide) onto rubberwood fibre," *BioResources* 6(4), 5110-5120.

Md. Yunos, N. S. H., Baharuddin, A. S., Md. Yunos, K. F., Nazli Naim, M., and Nishida, H. (2012). "Physicochemical property changes of oil palm mesocarp fibers treated with high-pressure steam," *BioResources* 7(4), 5983-5994.

Mohanty, A. K., Misra, M., Drzal, L. T., Selke, S. E., Hante, B. R., and Hinrichsen, G. (2005). *Natural Fibers, Biopolymers, and Biocomposites*, A. K. Mohanty, M. Misra, and L. T. Drzal (eds.), CRC/Taylor & Francis, Boca Raton, FL.

Myers, R. H., Montgomery, D. C., and Anderson-Cook, C. M. (2009). *Response Surface Methodology: Process and Product Optimization Using Designed Experiments, 3rd ed.*, D. J. Balding, N. A. C. Cressie, G. M. Fitzmaurice, I. M. Johnstone, G. Molenberghs, D. W. Scott, A. F. M. Smith, R. S. Tsay, and S. Weisberg (eds.), John Wiley & Sons, New York.

Qin, L., Qiu, J., Liu, M., Ding, S., Shao, L., Lu, S., Zhang, G., Zhao, Y., and Fu, X. (2011). "Mechanical and thermal properties of poly(lactic acid) composites with rice straw fiber modified by poly(butyl acrylate)," *Chem. Eng. J.* 166(2), 772-778.

Raju, G., Ratnam, C. T., Ibrahim, N. A., Rahman, M. Z. A., and Wan-Yunus, W. M. Z. (2007). "Graft copolymerization of methyl acrylate onto oil palm empty fruit bunch (OPEFB) fiber," *Polym-Plast. Technol.* 46(10), 949-955.

Razali, M. A. A., Sanusi, N., Ismail, H., Othman, N., and Ariffin, A. (2012). "Application of response surface methodology (RSM) for optimization of cassava starch grafted polyDADMAC synthesis for cationic properties," *Starch – Starke* 64(12), 935-943.

Sayyah, S. M., Khaliel, A. B., and Mohamed, E. H. (2013). "Enhancing water resistance of paper by graft copolymerization reaction," *J. Appl. Polym. Sci.* 127(6), 4446-4455.

Singha, A. S., and Thakur, V. K. (2008). "Fabrication and study of lignocellulosic *Hibiscus Sabdariffa* fiber reinforced polymer composites," *BioResources* 3(4), 1173-1186.

Singha, A. S., and Thakur, V. K. (2009). "Study of mechanical properties of urea-formaldehyde thermosets reinforced by pine needle powder," *BioResources* 4(1), 292-308.

Singha, A. S., and Thakur, V. K. (2010). "Synthesis and characterization of short *Grewia optiva* fiber-based polymer composites," *Polym. Composite.* 31(3), 459-470.

Soo, M. C., Wan Daud, W. R., and Leh, C. P. (2012). "Improvement of recycled paper's properties for the production of braille paper by impregnation with low grade cellulose acetate: Optimization using response surface methodology (RSM)," *BioResources* 7(4), 5333-5345.

Sreekala, M. S., Kumaran, M. G., and Thomas, S. (1997). "Oil palm fibers: Morphology, chemical composition, surface modification, and mechanical properties," *J. Appl. Polym. Sci.* 66(5), 821-835.

Thakur, V. K., Singha, A. S., and Misra, B. N. (2011). "Graft copolymerization of methyl methacrylate onto cellulosic biofibers," *J. Appl. Polym. Sci.* 122(1), 532-544.

Thakur, V. K., Singha, A. S., and Thakur, M. K. (2012). "Rapid synthesis of MMA grafted pine needles using microwave radiation," *Polym-Plast. Technol.* 51(15), 1598-1604.

Thakur, V. K., Singha, A. S., and Thakur, M. K. (2012). "Synthesis of natural cellulose–based graft copolymers using methyl methacrylate as an efficient monomer," *Adv. Polym. Technol.* 32(S1), E741-E748.

Thakur, V. K., Thakur, M. K., and Gupta, R. K. (2013). "Graft copolymers from cellulose: Synthesis, characterization and evaluation," *Carbohyd. Polym.* 97(1), 18-25.

Yang, H., Yan, R., Chen, H., Lee, D. H., and Zheng, C. (2007). "Characteristics of hemicellulose, cellulose and lignin pyrolysis," *Fuel* 86(12-13), 1781-1788.

Article submitted: June 3, 2013; Peer review completed: July 9, 2013; Revised version received: July 19, 2013; Accepted: August 22, 2013; Published: August 28, 2013.